

[Ni^{II}(3-OMe-salophene)]: A Potent Agent with Antitumor Activity

Soo-Young Lee,[†] Annegret Hille,[‡] Corazon Frias,[§] Benjamin Kater,[†] Birgit Bonitzki,[†] Stefan Wöflfl,^{||} Heike Scheffler,[‡] Aram Prokop,^{†,§} and Ronald Gust^{*,‡,⊥}

[†]Department of Pediatric Oncology/Hematology, University Medical Center Charité, Berlin, Germany, [‡]Institute of Pharmacy, Freie Universität Berlin, Berlin, Germany, [§]Department of Pediatric Oncology, Children's Hospital of the City of Cologne, Cologne, Germany, ^{||}Institute of Pharmacy and Molecular Biotechnology, Im Neuenheimer Feld 364, 69120 Heidelberg, Germany, and [⊥]Department of Pharmaceutical Chemistry, Institute of Pharmacy, University of Innsbruck, Innrain 52a, A-6020 Innsbruck, Austria

Received April 14, 2010

In this study, we investigated the anticancer properties of methoxy-substituted nickel(II)(salophene) derivatives. We demonstrated that the most active complex [Ni^{II}(3-OMe-salophene)] is not necrotic in Burkitt-like lymphoma cells (BJAB) and human B-cell precursor cells (Nalm-6). [Ni^{II}(3-OMe-salophene)] inhibited proliferation and induced apoptosis in a concentration dependent manner, giving evidence for the involvement of CD95 receptor-mediated, extrinsic pathway. Furthermore, [Ni^{II}(3-OMe-salophene)] overcame vincristine drug resistance in BJAB and Nalm-6 cells.

Introduction

Medicinal applications of inorganic chemistry are varied, encompassing many aspects of the introduction of metal ions into the body for therapeutic effect.^{1,2} The ligands of organometallic complexes are needed to ensure cellular uptake culminating in precisely targeted particular tissues or enzymes. Additionally, biomolecular interactions of these metal-based drugs are determined by the electrochemical and kinetic variables of the respective central atom. The characteristics of diverse non-platinum-containing metal compounds and their use and/or putative mode of action in modern cancer treatment are described in several review articles (e.g., see refs 3 and 4). Recently we showed that especially the iron(salophene) complexes have increased anti-tumor activity in MCF-7 and MDA-MB-231 breast as well as HT-29 colon cancer cells.⁵ Furthermore, we demonstrated the importance of the methoxy group in the salicylidene moieties of the salophene ligand. The results obtained in a time-dependent chemosensitivity test clearly confirmed the correlation between cytotoxicity of the complexes and the position of the methoxy substituents; the best cell growth inhibitory effects were obtained with the complexes bearing the electron donating group in positions ortho and para to the imine moiety. Recently, we showed that [Fe^{III}(salophene)Cl] induced mitochondrial apoptosis in a concentration-dependent manner and overcame resistance to the conventional therapeutics daunorubicine and vincristine.^{6,7}

Taking into account that some nickel (Schiff base) complexes reveal their antitumor activity via DNA adduct formation and double strand breaks, promoting selective oxidation of Z-DNA, depleting glutathione and protein sulfhydryl groups, we focused our attention on the biological properties of methoxy-substituted nickel(salophene) complexes, too.^{8–12}

Despite all these different modes of action, data about cell selectivity and resistance overcome of nickel(salophene) complexes are missing. Here we describe antiproliferative effects of methoxy-substituted nickel(II)(salophene) complexes. The most active compound [Ni^{II}(3-OMe-salophene)] was further investigated for its ability to induce programmed cell death and to overcome resistance to the common therapeutic drug vincristine in lymphoma and leukemia cells. Furthermore, we demonstrated that the [Ni^{II}(3-OMe-salophene)]-induced apoptosis is mediated by the CD95 receptor and is dependent on the expression of the Fas-associated protein with death domain (FADD⁹) and the second mitochondria activator of caspases (smac), thus implying that the anticancer activity is involved in the extrinsic apoptotic pathway.

Results

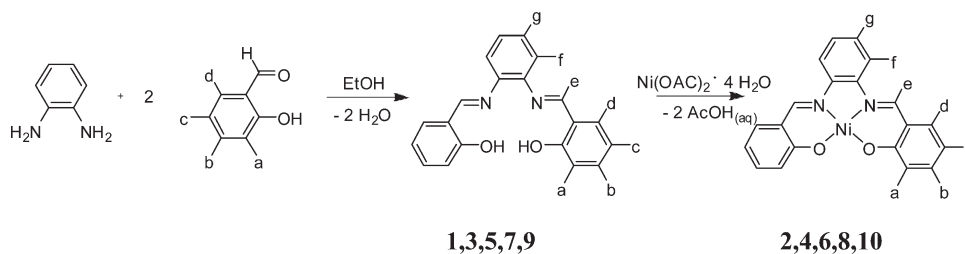
Synthesis and Characterization of the Test Compounds by ¹H NMR Spectroscopy. The methoxy-substituted salophene ligands were synthesized as already described.^{5,7} Reaction of the respective ligand with Ni(II) acetate tetrahydrate (Table 1) yielded the desired Ni(II)(salophene) complex in sufficient purity.

The characterization of salophene ligands and Ni(II) complexes were performed by using ¹H NMR spectroscopy (Figures 1). Nickel is one of the late row transition metals forming with salophene-like ligands square planar diamagnetic Schiff base complexes suitable for NMR investigation.

As depicted in Figure 1A, the ligands **5** and **9** showed the resonance peaks of H_a and H_c at nearly the same frequency with an upfield shift, indicating high electron density at these

*To whom correspondence should be addressed. Address: Department of Pharmaceutical Chemistry, Institute of Pharmacy, University of Innsbruck, Innrain 52a, A-6020 Innsbruck, Austria. Phone: +43 512 507 5245. Fax: +43 512 507 2940. E-mail: ronald.gust@uibk.ac.at.

⁹Abbreviations: ALL, acute lymphoblastic leukemia; DMEM, Dulbecco's modified Eagle's medium; FACS, fluorescence activated cell sorting; FADD, Fas-associated protein with death domain; INT, 2-[4-iodophenyl]-3-[4-nitrophenyl]-5-phenyltetrazolium chloride; JC-1, 5,5',6,6'-tetrachloro-1,1,3,3'-tetraethylbenzimidazolylcarbocyanine iodide; LDH, lactate dehydrogenase; PBS, phosphate buffered saline; smac, second mitochondria activator of caspases; Vcr, vincristine.

Table 1. Synthesized Compounds with e, f, and g as protons

a	b	c	d	compd	no.	IC ₅₀ (μM)
H	H	H	H	salophene	1	
H	H	H	H	[Ni ^{II} salophene]	2	7.98
OMe	H	H	H	3-O-Me-salophene	3	
OMe	H	H	H	[Ni ^{II} (3-O-Me-salophene)]	4	0.36
H	OMe	H	H	4-O-Me-salophene	5	
H	OMe	H	H	[Ni ^{II} (4-O-Me-salophene)]	6	34.2
H	H	OMe	H	5-O-Me-salophene	7	
H	H	OMe	H	[Ni ^{II} (5-O-Me-salophene)]	8	> 50
H	H	H	OMe	6-O-Me-salophene	9	
H	H	H	OMe	[Ni ^{II} (6-O-Me-salophene)]	10	8.85

positions. Additionally, these signals of **5** were separated as a double–doublet (H_c) and doublet (H_a) while those of **9** were superimposed to a quasi triplet. After coordination (compound **10**, Figure 1B), H_a and H_c were well separated because of a strong high field shift of H_a, whereas the signals of H_a and H_c of compound **6** remained nearly unchanged.

The resonance signals assigned to H_f and H_g of the ligands appeared at 7.4–7.5 ppm, irrespective of the substitution pattern, indicating that the electron density distribution within the phenylene moiety was not significantly affected by the position of the OCH₃ substituent in the salicylidene ring. After coordination of the ligands, however, H_f was characteristically shifted to lower field (from about 7.4 to 8–8.2 ppm). Interestingly, both resonance signals occurred at the same frequencies of 8.16 ppm (H_f) and 7.35 ppm (H_g) in the spectra of the complexes **2**, **4**, and **8**.

In Vitro Chemosensitivity Assay. Anticancer activity of the nickel(II) complexes **2**, **4**, **6**, **8**, and **10** against MCF-7 mammary carcinoma cells was evaluated in a time-dependent (see Figure S1 of Supporting Information) and concentration-dependent (IC₅₀ determination; see Table 1) crystal violet assay. Whereas all ligands were inactive (data not shown), the position of the methoxy substituent determined the potency of the respective nickel complex.

The unsubstituted (**2**) and the 6-OCH₃ derivative (**10**) caused low growth inhibitory effects (50–60% reduction) at 1 μM. A shift of the OCH₃ group from position 6 to 5 or 4 terminated the activity at this concentration, while a shift to position 3 led to an analogue (**4**, [Ni^{II}(3-O-Me-salophene)]) with cytotoxic properties (see Figure S1). It already blocked cell growth after an incubation time of 60 h.

For a better comparison of the antitumor potency, the IC₅₀ values were calculated after an incubation time of 72 h (Table 1). At that time all complexes reached their maximal growth inhibitory effects (see Figure S1), which increased in the following order: **8** (5-OCH₃, IC₅₀ > 50 μM) < **6** (4-OCH₃, IC₅₀ = 34.2 μM) < **10** (6-OCH₃, IC₅₀ = 8.85 μM) ~ **2** (H, IC₅₀ = 7.98 μM) ≪ **4** (3-OCH₃, IC₅₀ = 0.36 μM).

Because of its outstanding cytotoxicity, [Ni^{II}(3-O-Me-salophene)] was selected for further biological investigations.

Exclusion of Necrotic Effects. Many cytotoxic substances cause undesired necrotic cell death which is characterized by

membrane damage and the early release of lactate dehydrogenase (LDH). In order to exclude such an unspecific cytotoxic effect, we determined the amount of extracellular LDH in Burkitt-like lymphoma cells (BJAB) by incubating the cells with various concentrations (0–20 μM) of the complex [Ni^{II}(3-O-Me-salophene)] for 3 h and measuring the LDH release into the culture medium via ELISA detection. As depicted in Figure 2, no significant LDH release could be detected after 3 h of incubation with the agent. It is assumed that necrosis does not have a significant impact on the potency of [Ni^{II}(3-O-Me-salophene)].

Induction of Apoptosis by [Ni^{II}(3-O-Me-salophene)]. [Ni^{II}(3-O-Me-salophene)] showed efficient antiproliferative effects in BJAB cells. As gauged from Figure 3, cell proliferation could be significantly decreased in a concentration-dependent manner. To further quantify the [Ni^{II}(3-O-Me-salophene)]-induced induction of apoptosis, we exposed BJAB cells to the drug at different concentrations for 72 h and analyzed DNA fragmentation by flow cytometric determination via fluorescence activated cell sorting (FACS). The data, shown in Figure 4, verify specific dose-dependent induction of apoptosis with a half-maximum concentration of about 10 μM.

Involvement of the Mitochondrial Pathway in the Induction of Apoptosis. In order to determine the involvement of the mitochondrial activation was measured by performing a JC-1 (5,5',6,6'-tetrachloro-1,1,3,3'-tetraethylbenzimidazolylcarbocyanine iodide) assay.¹³ For this purpose BJAB cells were incubated with [Ni^{II}(3-O-Me-salophene)] for 48 h, followed by staining the treated cells with the fluorescence dye JC-1 and quantification of the mitochondrial permeability via flow cytometric determination of cells with declined fluorescence. Our investigations revealed a minimal loss of the mitochondrial membrane potential at higher concentrations, thus indicating that the mitochondrial pathway does not play a very important role in [Ni^{II}(3-O-Me-salophene)]-induced apoptosis (Figure 5).

Induction of Apoptosis by [Ni^{II}(3-O-Me-salophene)] in Vincristine-Resistant Leukemia and Lymphoma Cell Lines. The development of resistance to various conventional chemotherapeutic drugs remains a major component in the failure of chemotherapy. Therefore, the effect of [Ni^{II}(3-O-Me-salophene)]

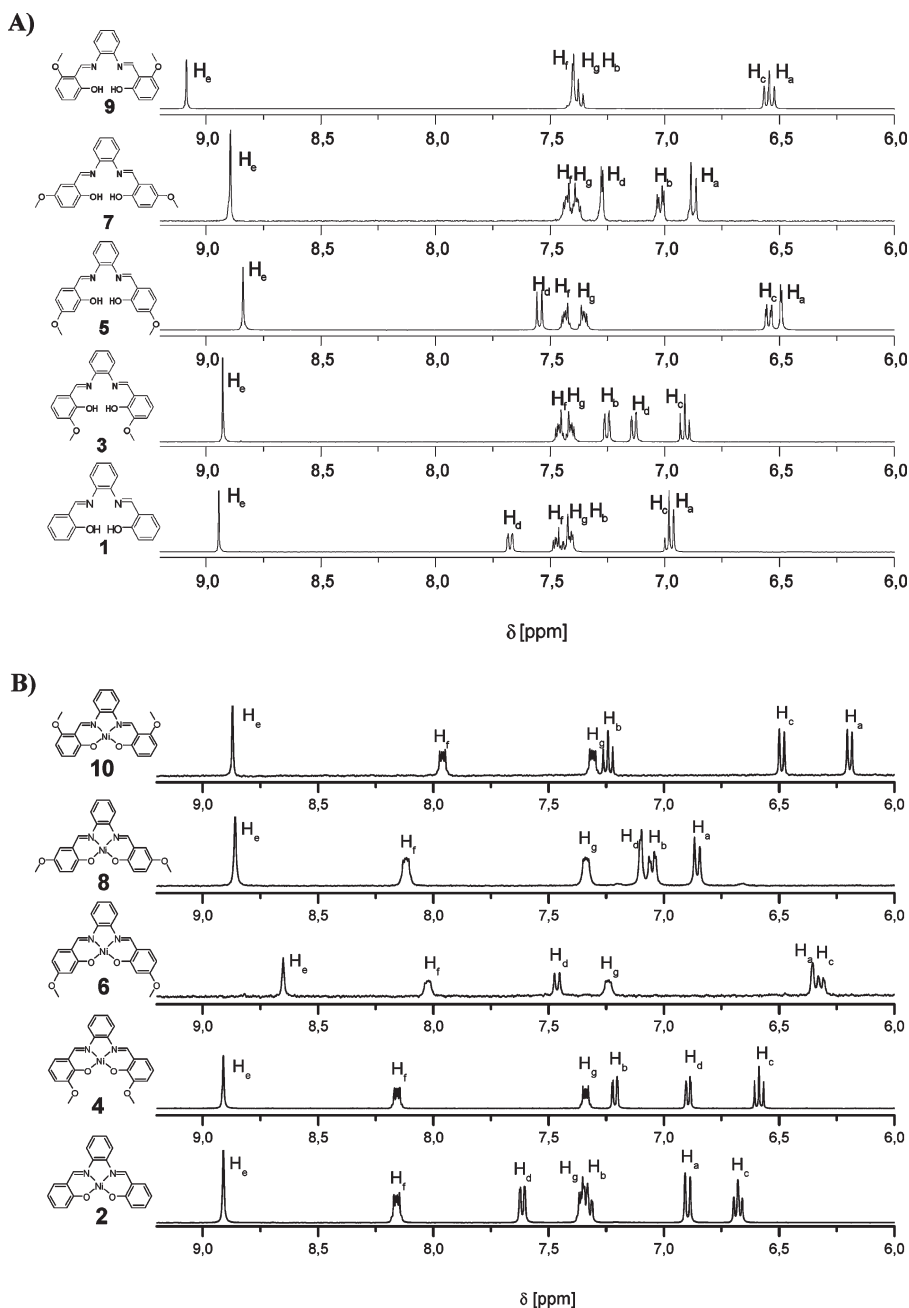


Figure 1. (A) ^1H NMR of the ligands 1, 3, 5, 7, and 9. (B) ^1H NMR of the nickel(II) complexes 2, 4, 6, 8, 10.

on vincristine (Vcr) resistant leukemia and lymphoma cell lines was tested. After treatment of regular leukemia cells (Nalm-6) and lymphoma cells (BJAB) and a Vcr modification of both cell lines for 72 h, the apoptosis induction was determined by flow cytometric measurements. As depicted in Figure 6, $[\text{Ni}^{\text{II}}(3\text{-OMe-salophene})]$ induced higher apoptosis in the resistant cells compared to the control cells. Thus, it can be assumed that the agent was capable of overcoming drug resistance in Vcr-resistant leukemia and lymphoma cells.

Involvement of the Extrinsic Pathway in $[\text{Ni}^{\text{II}}(3\text{-OMe-salophene})]$ -Induced Apoptosis. As described before, the mitochondrial pathway does not seem to play an important role in the induction of apoptosis, since there was no significant loss of the mitochondrial membrane potential observed. To emphasize the suggestion that the $[\text{Ni}^{\text{II}}(3\text{-OMe-salophene})]$ -induced apoptosis mainly follows the extrinsic pathway, we used Jurkat cells (human T cell leukemia cell line) over-

expressing smac, a proapoptotic mitochondrial protein that is released during the intrinsic apoptotic pathway. As depicted in Figure 7, the $[\text{Ni}^{\text{II}}(3\text{-OMe-salophene})]$ -induced cell death turned out to be independent of the expression of the proapoptotic intrinsic factor smac.

Additionally, the Fas-associated death domain dependence was investigated to further prove if the alternative extrinsic pathway takes part. In the extrinsic pathway binding of the Fas ligand to Fas/CD95 activates the apoptotic program by recruiting a FADD adaptor, finally leading to DNA fragmentation.¹⁴ Using BJAB cells overexpressing a dominant-negative FADD (FADD-dn) mutant, we could show that these cells underwent apoptosis to a lower level than the control cell line (BJAB mock), revealing that the DNA fragmentation was significantly influenced by FADD-dn overexpression, which in turn indicates that $[\text{Ni}^{\text{II}}(3\text{-OMe-salophene})]$ -induced cell death proceeds dependently of CD95/Fas signaling (Figure 8).

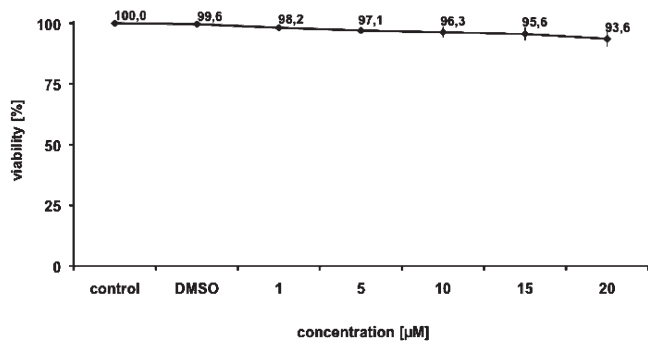


Figure 2. Quantification of lactate dehydrogenase (LDH) release. To evaluate necrotic properties of $[\text{Ni}^{\text{II}}(3\text{-OMe-salophene})]$, BJAB cells were treated with different concentrations of $[\text{Ni}^{\text{II}}(3\text{-OMe-salophene})]$ for 3 h. Viability of the cells was determined by LDH release through photometrical measurement via ELISA reader. LDH activity of lysed cells was used as a 100% control. Values are given as % of control \pm SD ($n = 3$).

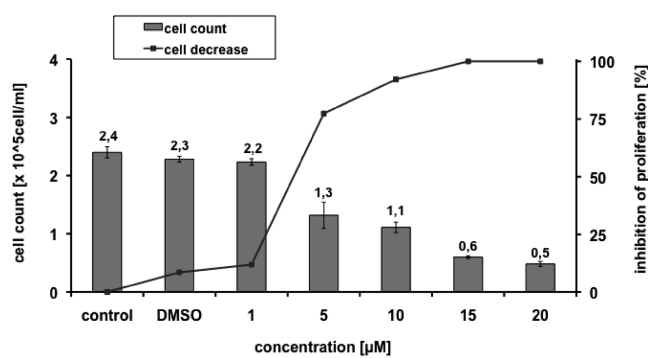


Figure 3. Antiproliferative effect of $[\text{Ni}^{\text{II}}(3\text{-OMe-salophene})]$ in BJAB cells. Inhibition of cell proliferation in a concentration-dependent manner after treatment with $[\text{Ni}^{\text{II}}(3\text{-OMe-salophene})]$ for 24 h as measured by a Casy cell counter system. Bars indicate the number of cells after 24 h of incubation in units of 10^5 cells $\text{mL}^{-1} \pm$ SD ($n = 3$). The line chart indicates the inhibition of cell proliferation as % of the control.

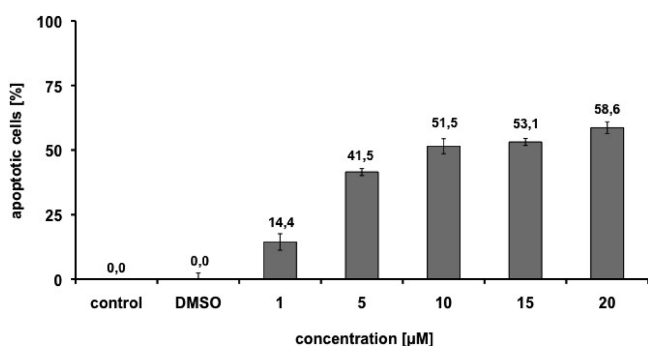


Figure 4. Apoptosis induction in BJAB cells after treatment with different concentrations of $[\text{Ni}^{\text{II}}(3\text{-OMe-salophene})]$. Nuclear DNA fragmentation was measured after 72 h of incubation via flow cytometric analysis by determining the hypodiploid DNA. Data are given as % hypodiploidy (subG1) \pm SD ($n = 3$), which reflects the number of apoptotic cells.

Discussion

Despite the improved outcome of patients with relapsed acute lymphoblastic leukemia (ALL), chemotherapy failure due to cellular drug resistance remains a leading problem in pediatric oncology. The inhibition of proliferation and the

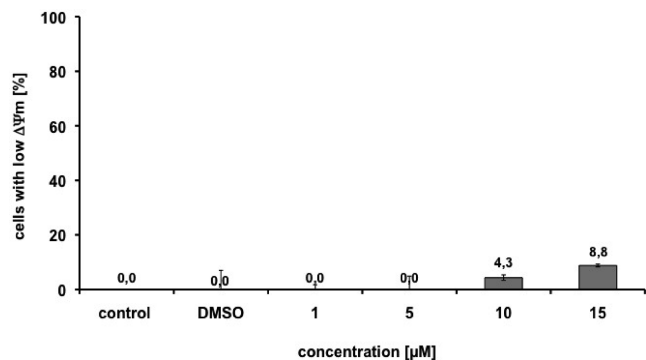


Figure 5. Influence of $[\text{Ni}^{\text{II}}(3\text{-OMe-salophene})]$ on the mitochondrial membrane potential. After 48 h of incubation of BJAB cells with $[\text{Ni}^{\text{II}}(3\text{-OMe-salophene})]$ the mitochondrial permeability transition was measured by flow cytometric analysis. Values of the mitochondrial permeability transition are given as the fraction of cells with decreased membrane potential ($\Delta\Psi_m$) in % \pm SD ($n = 3$).

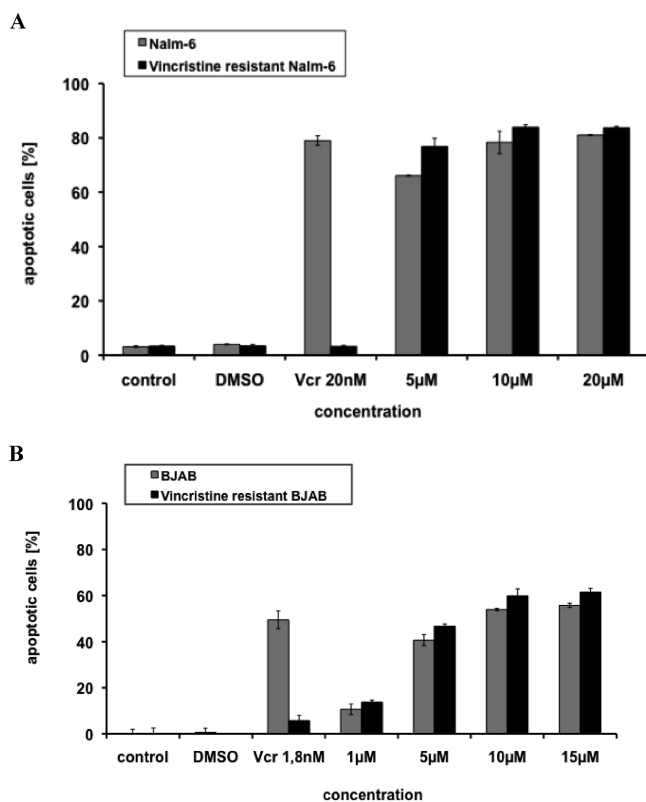


Figure 6. Apoptosis induced by $[\text{Ni}^{\text{II}}(3\text{-OMe-salophene})]$ in vincristine-resistant leukemia (Nalm-6) and lymphoma (BJAB) cells. Apoptosis was determined by DNA fragmentation in regular leukemia and lymphoma cells as well as in (A) Vcr-resistant Nalm-6 cells and (B) Vcr-resistant BJAB cells after an incubation period of 72 h with various concentrations of the indicated drug. Data are given as percentage hypodiploidy (subG1) \pm SD ($n = 3$), which reflects the number of apoptotic cells.

induction of apoptosis in tumor cells are known to be the major therapeutic mechanisms of anticancer drugs, since a deregulation of both processes causes malignant diseases.¹⁵

We already demonstrated the cytotoxic potential of the Schiff base iron complex $[\text{Fe}^{\text{III}}(\text{salophene})\text{Cl}]$ in vitro and ex vivo and illustrated its excellent ability to overcome multiple drug resistance. Treatment of BJAB lymphoma cells with $[\text{Fe}^{\text{III}}(\text{salophene})\text{Cl}]$ led to a concentration-dependent inhibition of proliferation up to 100%. A significant loss of the

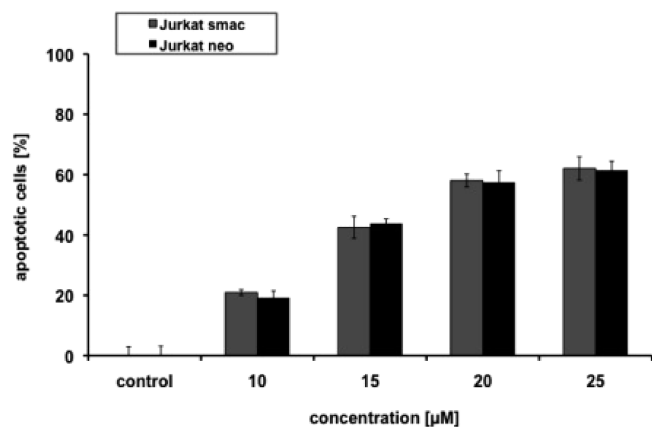


Figure 7. Impairment of overexpression of proapoptotic smac in human T cell leukemia cells (Jurkat) on $[\text{Ni}^{\text{II}}(3\text{-OMe-salophene})]$ -induced DNA fragmentation. By use of the cell line Jurkat smac, overexpressing the proapoptotic intrinsic factor smac, DNA fragmentation was measured by flow cytometric analysis after 72 h of incubation with $[\text{Ni}^{\text{II}}(3\text{-OMe-salophene})]$. Data are given as percentage hypodiploidy (sub-G1) \pm SD ($n = 3$), which reflects the number of apoptotic cells. As a control, vector-transfected Jurkat cells (Jurkat neo) were used.

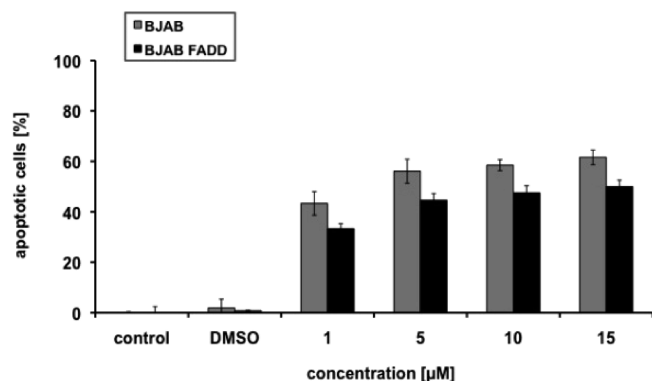


Figure 8. Impairment of overexpression of dominant-negative FADD in BJAB cells on $[\text{Ni}^{\text{II}}(3\text{-OMe-salophene})]$ -induced DNA fragmentation. After exposure of vector-transfected or FADD dn-transfected BJAB cells to $[\text{Ni}^{\text{II}}(3\text{-OMe-salophene})]$ for 72 h, DNA fragmentation was measured. Data are given as percentages of cells with hypodiploid DNA \pm SD ($n = 3$).

mitochondrial membrane potential in lymphoma cells indicated the involvement of the intrinsic mitochondrial pathway. Specific apoptotic cell death was detected for leukemia (Nalm-6) and lymphoma cells (BJAB) via DNA fragmentation. We further confirmed the up- and down-regulation of various apoptosis relevant genes via real-time PCR and an overcoming of drug resistance against vincristine- and daunorubicine-resistant Nalm-6 cells.

Introduction of OCH_3 into the salicylidene moieties modified the growth inhibitory potency. If the substituent is located in a position ortho or para to the phenolic oxygen, the activity will be reduced by half while the attachment at the meta-position increased the growth inhibitory effects. In each case, however, a steep concentration–response relation was observed.

In addition to these studies we verified the importance of the transition metal on controlling cancer cell proliferation of $[\text{Fe}^{\text{III}}(\text{salophene})\text{Cl}]$. As soon as the iron central atom was exchanged by nickel(II), cell growth inhibition and apoptosis induction were diminished, clearly pointing out the impor-

tance of the transition metal on the biological properties of the respective complex and the involvement of the metal in the mode of action.

In this structure–activity relationship study we could show that methoxy groups at the salicylidene moiety of $[\text{Ni}^{\text{II}}(\text{salophene})]$ modified the biological properties more efficiently. On the one hand, the introduction at the 4- or 5-position terminated the effects at the MCF-7 cell line nearly completely. The methoxy substituent at position 6 did not change the activity compared to the unsubstituted $[\text{Ni}^{\text{II}}(\text{salophene})]$ complex. On the other hand, a substitution at position 3 led to a compound with outstanding cytotoxicity. At the MCF-7 cell line, $\text{IC}_{50} = 0.34 \mu\text{M}$ was calculated, which is even lower than that of the reference cisplatin ($\text{IC}_{50} = 2.2 \mu\text{M}$). Therefore, $[\text{Ni}^{\text{II}}(3\text{-OMe-salophene})]$ was selected for detailed biological studies. This complex induced, in contrast to $[\text{Fe}^{\text{III}}(\text{salophene})\text{Cl}]$, apoptosis in a FADD- and smac-dependent manner and was accompanied by a minor loss of the mitochondrial membrane potential, thus indicating that $[\text{Ni}^{\text{II}}(3\text{-OMe-salophene})]$ efficiently triggers the extrinsic pathway of apoptosis. Furthermore, $[\text{Ni}^{\text{II}}(3\text{-OMe-salophene})]$ overcomes vincristine resistance in leukemia and lymphoma cells.

Conclusions

We demonstrated in this paper that $[\text{Ni}^{\text{II}}(3\text{-OMe-salophene})]$ constitutes a novel lead structure with remarkably high levels of apoptosis induction in leukemia and lymphoma cells and promising anticancer activities in drug resistant cell lines.

Experimental Section

General. Chemicals were obtained from Sigma Aldrich (Germany) and used without further purification. The following instrumentation was used: ^1H NMR, Bruker ADX 400 spectrometer at 400 MHz (internal standard, TMS); EI-MS spectra, CH-7A Varian (70 eV); IR spectra (KBr pellets), Perkin-Elmer model 580 A. Elemental C, H, N analyses were carried out with a Perkin-Elmer 240 B and 240 C elemental analyzer. The purity of all synthesized substances was confirmed by elemental analysis. All complexes reported in the manuscript have a purity of $> 95\%$.

Synthesis. Salophene (**1**), $[\text{Ni}^{\text{II}}(\text{salophene})]$ (**2**), and the methoxy-substituted salophene ligands **3**, **5**, **7**, and **9** were prepared as described elsewhere.^{5,7}

General Procedure for the Synthesis of the Complexes 4, 6, 8, 10. The respective ligand was dissolved in ethanol (10 mL) and heated to reflux in the presence of 1.5 equiv of $\text{Ni}(\text{OAc})_2 \cdot 4\text{H}_2\text{O}$ in ethanol (5 mL). After 1–2 h, the mixture was allowed to cool to room temperature and the solid obtained was filtered off, washed with ethanol, and dried in vacuum.

$[\text{Ni}^{\text{II}}(3\text{-OMe-salophene})]$ 4. Compound **4** was obtained from *N,N'*-bis(3-methoxysalicylidene)-1,2-phenylenediamine and 1.5 equiv of $\text{Ni}(\text{OAc})_2 \cdot 4\text{H}_2\text{O}$ as a red-black solid. Yield: 237.33 mg (0.57 mmol, 72%). ^1H NMR (DMSO- d_6): $\delta = 8.91$ (s, 2H, H_e), 8.17–8.14 (AA'XX', 2H, H_f , $^3J = 9.6$ Hz, $^4J = 2.9$ Hz), 7.35–7.33 (AA'XX', 2H, H_g , $^3J = 9.5$ Hz, $^4J = 3.0$ Hz), 7.22–7.20 (dd, 2H, H_b , $^3J = 6.9$ Hz, $^4J = 1.4$ Hz), 6.90–6.89 (dd, 2H, H_d , $^3J = 7.4$ Hz, $^4J = 1.1$ Hz), 6.61–6.57 (dd, 2H, H_c , $^3J = 7.9$ and 7.8 Hz), 3.76 (s, 6H, $-\text{OCH}_3$). IR (KBr): ν [cm^{-1}] = 1608 s, 1540 s, 1247 s, 1199 s, 740 m. MS (EI, 100 °C): m/z (%) = 432 (100) $[\text{M}^+]$. Anal. (C₂₂H₁₈N₂O₄Ni) C, H, N.

Stability of Stock Solution. For stability evaluations in DMSO- d_6 the nickel(II) complexes **2** and **6** were dissolved. The proton resonance of this solution was measured within a week of freezing–thawing cycles. Because no changes were observed in the resulting ^1H NMR spectra, the respective stock solution of the nickel(II) complexes in DMSO could be stored at -20 °C (data not shown).

Biological Methods. Cell Culture Conditions and in Vitro Chemosensitivity Assay. The anticancer activity of all compounds against MCF-7 breast cancer cells was determined as described previously.⁵ Prior to use, the respective DMSO stock solution was diluted with DMEM to obtain the desired concentration. The final DMSO concentration amounted to 0.1%. The following cell lines were used: BJAB (Burkitt like lymphoma cells), mock and FADD transfected cells; Nalm-6 (human B cell precursor leukemia cells); Jurkat (human T cell leukemia cells), neo/smac-transfected cells; vincristine-resistant BJAB and Nalm-6. The cells were subcultured every 3–4 days by dilution of the cells to 1×10^5 /mL. All experiments were performed in DMEM or RPMI 1640 (GIBCO, Invitrogen) supplemented with 10% heat inactivated fetal calf serum, 100 U/mL penicillin, 100 μ g/mL streptomycin, and 0.56 g/L L-glutamine. Twenty-four hours before the assay was set up, cells were cultured at a concentration of 3×10^5 /mL to attain standardized growth conditions. For apoptosis assays, the cells were then diluted to 1×10^5 /mL immediately before addition of [Ni^{II} (3-OMe-salophene)].

Measurement of Cell Death by LDH-Release Assay. Cytotoxicity of the different drugs was measured by the release of lactate dehydrogenase (LDH). After incubation with different concentrations of the agents for 3 h, LDH activity released by BJAB cells was measured in the cell culture supernatants using the cytotoxicity detection kit from Boehringer Mannheim (Mannheim, Germany). The supernatants were centrifuged at 1500 rpm for 5 min. An amount of 20 μ L of cell-free supernatants was diluted with 80 μ L of phosphate-buffered saline (PBS), and an amount of 100 μ L of reaction mixture containing 2-[4-iodophenyl]-3-[4-nitrophenyl]-5-phenyltetrazolium chloride (INT), sodium lactate, NAD⁺, and diaphorase were added. Then time-dependent formation of the reaction product was photometrically quantified at 490 nm. The maximum amount of LDH activity released by the cells was determined after lysis of the cells using 0.1% Triton X-100 in culture medium and set to represent 100% cell death.

Determination of Cell Concentration and Cell Viability. Cell viability was determined by using the “CASY cell counter + analyzer system” of Innovatis (Bielefeld, Germany). Settings were specifically defined for the requirement of the cells used. With this system the cell concentration can be analyzed simultaneously in three different size ranges; thus, cell debris, dead cells, and viable cells could be determined in one measurement. Cells were seeded at a density of 1×10^5 cells/mL and treated with different concentrations of [Ni^{II}(3-OMe-salophene)]; non-treated cells served as control. After a 24 h incubation period, cells were resuspended completely and 100 μ L of each well was diluted in 10 mL of CASYton (ready-to-use isotonic saline solution) for immediate automated counting.

Measurement of DNA Fragmentation. Apoptotic cell death was determined by a modified cell cycle analysis, which detects DNA fragmentation at the single cell level as described.¹⁶ Cells were seeded at a density of 1×10^5 cells/mL and treated with different concentrations of the agents. After a 72 h incubation period at 37 °C, cells were collected by centrifugation at 1500 rpm for 5 min, washed with PBS at 4 °C, and fixed in PBS/2% (v/v) formaldehyde on ice for 30 min. After fixation, cells were pelleted, incubated with ethanol/PBS (2:1, v/v) for 15 min, pelleted, and resuspended in PBS containing 40 μ g/mL RNase. RNA was digested for 30 min at 37 °C, after which the cells were pelleted again and finally resuspended in PBS containing 50 μ g/mL propidium iodide. Nuclear DNA fragmentation was quantified by flow cytometric determination of hypodiploid DNA. Data were collected and analyzed using a FACScan (Becton Dickinson, Heidelberg, Germany) equipped with CELL Quest software. Data are given in percent hypodiploidy (subG1), which reflects the number of apoptotic cells.

Annexin-V–Propidium Iodide Binding Assay. Cell death was determined by staining cells with Annexin-V-FITC and counter-

staining with propidium iodide. During apoptosis, the phospholipid phosphatidylserine is exposed to the outer leaflet of the plasma membrane. Annexin-V-FITC then binds to phosphatidylserine, leading to an increase in fluorescence.^{17,18} On the other hand, propidium iodide is excluded from cells with intact membranes. Propidium iodide positivity is therefore a sign of cell necrosis, whereas cells that are annexin-V-FITC positive but propidium negative are generally defined as apoptotic.¹⁹ For the annexin-V–propidium iodide assay, 1×10^5 cells were washed twice with ice cold PBS and then resuspended in a binding buffer (10 mM 4-(2-hydroxyethyl)-1-piperazineethanesulfonic acid/NaOH (pH 7.4), 140 mM NaCl, 2.5 mM CaCl₂) at 1×10^6 cells/mL. Next, 5 mL of annexin-V-FITC (BD Pharmingen, Heidelberg, Germany) and 10 μ L of 50 μ g/mL propidium iodide (Sigma-Aldrich, Taufkirchen, Germany) were added to the cells. Analyses were performed on a FACScan (Becton Dickinson, Heidelberg, Germany) using the CellQuest analysis software.

Acknowledgment. Financial support by the Deutsche Forschungsgemeinschaft (DFG-project FOR630) and the Dr. Kleist Foundation, Berlin, are gratefully acknowledged.

Supporting Information Available: Elemental analysis results of all complexes; time-dependent growth inhibition of MCF-7 cells; and experimental data of complexes **6**, **8**, and **10**. This material is available free of charge via the Internet at <http://pubs.acs.org>.

References

- (1) Kraatz, H. B.; Metzler-Nolte, N. *Medicinal Inorganic Chemistry. In Concepts and Models in Bioinorganic Chemistry*; Wiley-VCH: Weinheim, Germany, 2006; pp26–27.
- (2) Sadler, P. J. *Inorganic chemistry and drug design. Adv. Inorg. Chem.* **1991**, *36*, 1–48.
- (3) Ott, I.; Gust, R. Non platinum metal complexes as anti-cancer drugs. *Arch. Pharm. Chem. Life Sci.* **2007**, *340*, 117–126.
- (4) Schatzschneider, U.; Metzler-Nolte, N. New principles in medicinal organometallic chemistry. *Angew. Chem., Int. Ed.* **2006**, *45*, 1504–1507.
- (5) Hille, A.; Ott, I.; Kitanovic, A.; Kitanovic, I.; Alborzina, H.; Lederer, E.; Wöfl, S.; Metzler-Nolte, N.; Schäfer, S.; Sheldrick, W. S.; Bischof, C.; Schatzschneider, U.; Gust, R. [*N,N'*-Bis-(salicylidene)-1,2-phenylenediamine]metal complexes with cell death promoting properties. *J. Biol. Inorg. Chem.* **2009**, *14*, 711–725.
- (6) Hille, A.; Lee, S.-Y.; Kater, L.; Kater, B.; Jesse, P.; Kitanovic, I.; Wöfl, S.; Gust, R.; Prokop, A. [Fe^{III}(salophene)Cl], a potent iron salophene complex overcomes multiple drug resistance in lymphoma and leukemia cells. Unpublished results.
- (7) Hille, A.; Gust, R. Influence of methoxy groups on the antiproliferative effects of [Fe^{III}(salophene-OMe)Cl] complexes. Unpublished results.
- (8) Muller, J. G.; Kayser, L. A.; Paikoff, S. J.; Duarte, V.; Tang, N.; Perez, R. J.; Rokita, E. S.; Burrows, C. J. Formation of DNA adducts using nickel(II) complexes of redox-active ligands: a comparison of salene and peptide complexes. *Coord. Chem. Rev.* **1999**, *185–186*, 761–774.
- (9) Tang, N.; Muller, J. G.; Burrows, C. J.; Rokita, S. E. Nickel and cobalt reagents promote selective oxidation of Z-DNA. *Biochemistry* **1999**, *38*, 16648–16654.
- (10) Liang, F.; Wang, P.; Zhou, X.; Li, T.; Li, Z.; Lin, H.; Gao, D.; Zheng, C.; Wu, C. Nickel(II) and cobalt(II) complexes of hydroxyl-substituted triazamacrocyclic ligand as potential antitumor agents. *Bioorg. Med. Chem. Lett.* **2004**, *14*, 1901–1904.
- (11) Stohs, S. J.; Bagchi, D. Oxidative mechanisms in the toxicity of metal ions. *Free Radical Biol. Med.* **1995**, *18*, 321–336.
- (12) Reed, J. E.; Arnal, A. A.; Neidle, S.; Vilar, R. Stabilization of G-quadruplex DNA and inhibition of telomerase activity by square-planar nickel(II) complexes. *J. Am. Chem. Soc.* **2006**, *128*, 5992–5993.
- (13) Reers, M.; Smith, T. W.; Chen, L. B. J-Aggregate formation of a carbocyanine as a quantitative fluorescent indicator of membrane potential. *Biochemistry* **1991**, *30*, 4480–4486.
- (14) Nagata, S. Apoptosis by death factor. *Cell* **1997**, *88*, 355–365.
- (15) Herr, I. Cellular stress response and apoptosis in cancer therapy. *Blood* **2001**, *98*, 2603–2614.

- (16) Essmann, F.; Wieder, T.; Otto, A.; Müller, E. C.; Dörken, B.; Daniel, P. T. GDP dissociation inhibitor D4-GDI (Rho-GDI 2), but not the homologous Rho-GDI 1, is cleaved by caspase-3 during drug-induced apoptosis. *Biochem. J.* **2000**, *346*, 777–783.
- (17) Fadok, V. A.; Xue, D.; Henson, P. If phosphatidylserine is the death knell, a new phosphatidylserine-specific receptor is the bellringer. *Cell Death Differ.* **2001**, *8*, 582–587.
- (18) Schlegel, R. A.; Williamson, P. Phosphatidylserine, a death knell. *Cell Death Differ.* **2001**, *8*, 551–563.
- (19) Vermes, I.; Haanen, C.; Steffens-Nakken, H.; Reutelingsperger, C. A novel assay for apoptosis. Flow cytometric detection of phosphatidylserine expression on early apoptotic cells using fluorescein labelled annexin V. *J. Immunol. Methods* **1995**, *184*, 39–51.